SUPPORTING INFORMATION

Control of anisotropic self-assembly of gold nanoparticles coated with mesogens

Xiaobin Mang,[a] Xiangbing Zeng,*[a] Baijia Tang,[b] Feng Liu,[a] Goran Ungar,[a,c] Ruibin Zhang,[a] Liliana Cseh,[b] and Georg H. Mehl[b]

*[a] Department of Materials Science and Engineering, University of Sheffield, Sheffield S1 3JD, UK. *E-mail: x.zeng@shef.ac.uk*
[b] Department of Chemistry, University of Hull, Hull HU6 7RX, UK
[c] WCU program C2E2, School of Chemical and Biological Engineering, Seoul National University, Seoul, Korea

Contents

1 Synthesis of AuL3

1.1 Synthesis of the mesogenic thiol.

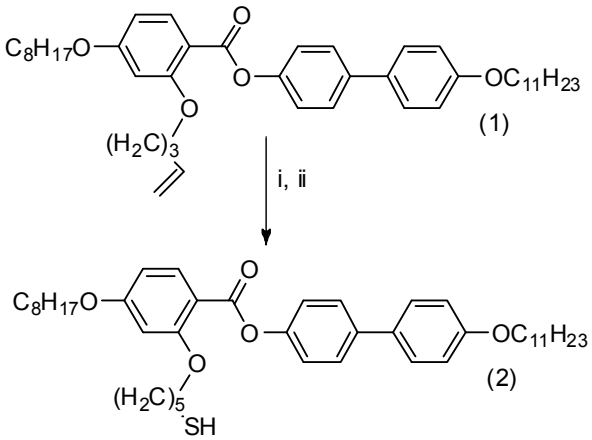

Scheme 1 *Reagents and conditions*: i, Ph_3SiSH (1.4 eq), AIBN, benzene, reflux 38h; ii, TFA (5 eq), room temperature, 30 min.

The compound **(1)** was prepared according to the literature.[1] The compound **(2)** was obtained in two steps: the first step is free-radical addition reaction induced by AIBN as initiator[2], and the second step involved a mild deprotection reaction, which was carried out using trifluoreacetic acid at room temperature. The thiol (2) was isolated by column chromatography (SiO_2, CH_2Cl_2/hexane = 4/1). Recrystallization from hexane yielded a white solid product in a yield of 37%.
Elemental Analysis (calc.) for $C_{43}H_{62}O_5S$, C, 74.7; H, 9.0; S, 4.6. Found: C, 75.0; H, 9.3; S, 4.4 %;
^{1}H-NMR (400 MHz in C_6D_6) δ 0.92(t, 6H, -CH_3), 1.04(t, 1H, -SH), 1.26-1.37(m, 34H, -CH_2-), 2.09(q, 2H, -CH_2-SH), 3.58-3.69(m, 6H, -O-CH_2-), 6.38(dd, 1H, $H_{ar.}$), 6.53(d, 1H, $H_{ar.}$), 6.91(dd, 2H, $H_{ar.}$), 7.29-7.43(m, 6H, $H_{ar.}$), 8.31(d, 1H, $H_{ar.}$),

1.2 Synthesis of AuL3

The synthetic procedure of gold clusters was based on procedure outlined in the literature.[3,4] The molar ratios used were : $HAuCl_4$: $(C_8H_{17})_4NBr$:thiol: $NaBH_4$ = 1:1.35:0.5:5.

To a solution of $HAuCl_4 \cdot 3H_2O$ (0.23 g, 0.66 mmol) in distilled water (25 ml) a solution of $(C_8H_{17})_4NBr$ (0.49 g, 0.90 mmol) in toluene (20 ml) was added. The bi-phasic solution was stirred rapidly until the gold ions were transferred to the organic phase. A mixture of the mesogenic thiol in toluene was added and the reaction mixture was stirred vigorously at room temperature for 10 minutes and then a freshly prepared solution of $NaBH_4$ (0.126 g, 3.33 mmol) in distilled water was added slowly so that the temperature of the mixture did not exceed 40 °C. The reaction mixture was stirred for 3h, a separation of the organic and the water phase was observed. The organic phase was concentrated under reduced pressure. Methanol was added (500ml) and the temperature was maintained at (-20°C) for 2h. The crude product was filtered on Celite and than washed with acetone to remove the excess thiol.

The product was dissolved in CH_2Cl_2 and precipitate with methanol. The thiol-derivatized gold nanoparticles AuL3 were isolated as black solid by centrifugation in a yield of 23.6 mg The NPs of the system AuL3 are air-stable and soluble in chloroform, toluene, dichloromethane, hexane, and other nonpolar solvents.

^{1}H-NMR 400 MHz, C_6D_6/δ [ppm]: 8,15 (H_{ar}); 7,56 (H_{ar}); 7,1 (H_{ar}); 6,5 (H_{ar}); 6,4 (H_{ar}); 3,75 (-O-CH_2-); 1,73 (-O-CH_2-C**H_2**-); 1,33 (-CH_2-); 0,96 (-CH_2-); 0,43 (-CH_3)
(All peaks very broad).

2 Powder SAXS data

2.1 AuL3

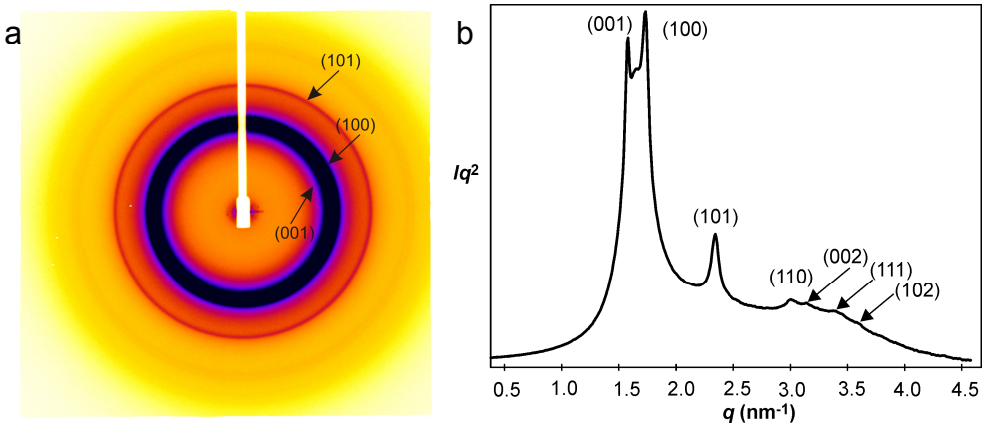

Figure S1. a) 2D powder SAXS pattern of AuL3 taken at 30ºC. b) The corresponding 1-d SAXS spectrum, radial scan of (a), Lorentz corrected.

Table S1. AuL3: Experimental and calculated *d*-spacings and diffraction intensities, measured at 30ºC, for the 3D hexagonal *P6/mmm* phase. Multiplicities and structure factor phase angles are also shown, as are calculated intensities from best-fit two-level model.

(*hkl*)	*d*-spacings (nm)		Intensities		Multi-plicity	Phase angle ϕ
	Exp.	Calc. *P6/mmm* *a*=4.10nm *c*=4.00nm	Exp.	Model D_{sphere}=1.79nm $\sqrt{\langle u^2 \rangle}$=0.84nm Δ = 4.46*		
(001)	4.00	4.00	42.4	44.0	2	0
(100)	3.55	3.55	100	99.1	6	0
(101)	2.66	2.65	68.8	68.8	12	0
(110)	2.06	2.05	6.9	6.4	6	0
(002)	2.00	2.00	1.3	1.6	2	0
(111)	1.83	1.82	10.1	3.9	12	0
(102)	1.74	1.74	2.1	2.8	12	0

* $\Delta = 100(\sum_i |I_i^{exp} - I_i^{calc}|)/\sum_i I_i^{exp}$ is the average difference between experimental and calculated diffraction intensities, in %.

2.2 AuL3C6

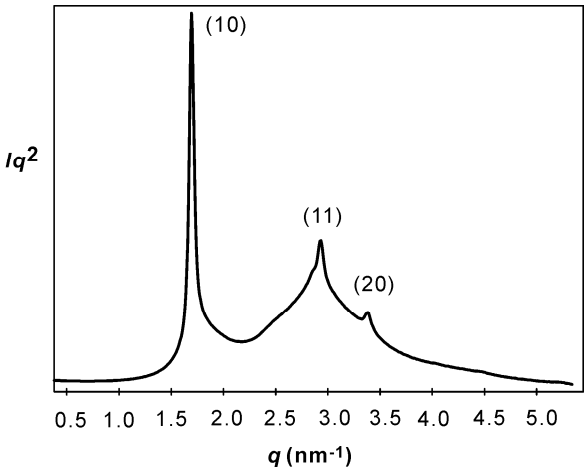

Figure S2. 1D SAXS spectrum of AuL3C6, radial scan of Figure 3b.

Table 2. AuL3C6: Experimental and calculated d-spacings and diffraction intensities, including multiplicities and structure factor phase angles of the 2D hexagonal phase at 30 ºC.

Peaks (*hk*)	*d*-spacings (nm)		Intensities		Multi-plicity	Phase angle ϕ
	Exp.	Calc. P6mm a=4.23nm	Exp.	Model D_{sphere}=1.62nm $\sqrt{\langle u^2 \rangle}$=0.69nm Δ = 2.8*		
(10)	3.66	3.66	100	100.0	6	0
(11)	2.12	2.11	16.1	16.2	6	0
(20)	1.83	1.83	7.6	6.1	6	0

* $\Delta = 100(\sum_i |I_i^{exp} - I_i^{calc}|)/\sum_i I_i^{exp}$

2.3 AuL3C12

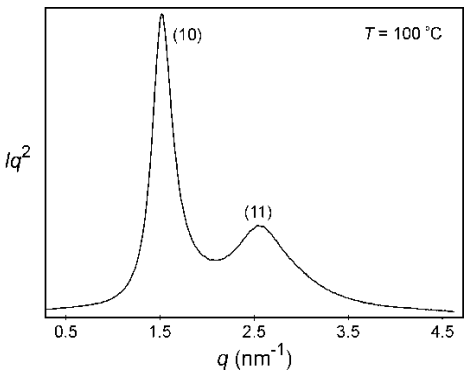

Figure S3. Powder SAXS spectrum of as prepared AuL3C12 recorded at 100 ºC.

Table 3. AuL3C12: Experimental and calculated d-spacings and diffraction intensities for the FCC phase, including multiplicities and structure factor phase angles. Calculated intensities from best-fit two-level model are also listed.

Peaks (*hkl*)	*d*-spacings (nm)		Intensities		Multi-plicity	Phase angle ϕ
	Exp.	Calc. $Fm\bar{3}m$ a=7.64nm	Exp.	Model D_{sphere}=2.27nm $\sqrt{\langle u^2 \rangle}$=0.44nm Δ= 5.36*		
(111)	4.42	4.41	100	100.0	8	0
(200)	3.83	3.82	53.7	59.6	6	0
(220)	2.70	2.70	45.1	43.5	12	0
(311)	2.31	2.30	34.1	37.0	24	0
(222)	2.21	2.21	11.7	9.0	8	0

$$* \Delta = 100(\sum_i |I_i^{exp} - I_i^{calc}|)/\sum_i I_i^{exp}$$

3 Reconstruction of Electron Density Maps

The electron density $\rho(xyz)$ in the unit cell of a periodic structure is linked to structure factor $F(hkl)$ by Fourier transform:

$$F(hkl) = \iiint \rho(xyz) \exp[-i2\pi(hx + ky + lz)]\, dxdydz \qquad (1)$$

Consequently, electron density can be reconstructed by the inverse Fourier transform once $F(hkl)$ is determined; thus

$$\rho(xyz) = \sum_{hkl} F(hkl) \exp\,[i2\pi(hx + ky + lz)] \qquad (2)$$

The observed x-ray diffraction intensity $I(hkl)$ is related to the structure factor $F(hkl)$

$$I(hkl) = k\,|F(hkl)|^2 \qquad (3)$$

Here k is a constant determined by the incident beam intensity, diffraction geometry, sample volume etc. As a result only $|F(hkl)|$ can be determined from diffraction intensity $I(hkl)$, but not its phase, leading to the well-known phase problem in x-ray crystallography.

Equation (2) can be rewritten as

$$\rho(xyz) = \sum_{hkl} |F(hkl)| \exp[i2\pi(hx+ky+lz)+\phi] \qquad (4)$$

The phase problem is much simplified if the structure is centrosymmetric, in which case $F(hkl)$ is always real and its phase ϕ can only be 0 or π. Liquid crystalline phases tend to have high symmetries due to the high mobility of the molecules, and the overwhelming majority are found to be centrosymmetric. This enables us to take a trial-and-error approach: the electron density maps are reconstructed with all possible phase combinations and the "correct" phase combination is chosen on the merit of the obtained electron density maps. This selection process is often helped by the knowledge of the system (the size of the molecules, volume ratios of different parts, isomorphous replacement experiments, study of homologous series of compounds, etc.). Simulation of diffraction pattern is also carried out, as described in the section below. In simulation the phase of $F(hkl)$ can be determined directly, and our choices of phase combinations have been verified in this way.

4 Simulation of Diffraction Patterns

The diffraction intensity can be expressed in terms of the lattice structure factor *S(q)* and the form factor $[F_{nano}(q)]^2$ of the nanoparticle. If GNP is considered as a sphere with uniform density, its form factor amplitude $F_{GNP}(q)$ is

$$F_{GNP}(q) = 3(\rho_{gold}-\rho_{org})V_{GNP}[\sin(qR)-qR\cos(qR)]/(qR)^3 \qquad (5)$$

Where ρ_{gold}, ρ_{org} are the electron density of the gold and the surrounding organic molecules respectively, V_{GNP} is GNP volume, q is reciprocal space scattering vector and R is the radius of the gold core. Considering the thermal fluctuation in the gold nanoparticle position, a Debye-Waller factor was included in the simulation. Therefore the final expression for the intensity in terms of the form factor is given by

$$I(q) = M(q)\, S(q)\, \exp(-\langle u^2\rangle q^2/3)[F_{GNP}(q)]^2 \qquad (6)$$

Where $\langle u^2\rangle$ is the mean square displacement of the centre position of gold nanoparticle, and *M(q)* is the multiplicity of the reflection.

Based on reconstructed electron density maps the structure model can be constructed, in which the positions of the nanoparticles in the unit cell can be defined. In all three phases considered, there is only one nanoparticle in the unit cell, hence the lattice factor $S(q)$ simply equals to 1.

5 AuL3C6 Textures under Polarized Microscope

The textures of the AuL3C6 under microscope between crossed polarizers (the polarization directions are horizontal and vertical respectively) are shown below. The sample was rotated and POM pictures are taken at 0°, 45° and 90°. A λ-plate, with slow axis along the northeast-southwest direction, was also used to determine the orientation of the fast and slow axis in the sample at each rotation angle. When the slow axis of a sample area is the same as the λ-plate, it will appear blue, and it will be reddish when the slow axis is perpendicular to that of the λ-plate.

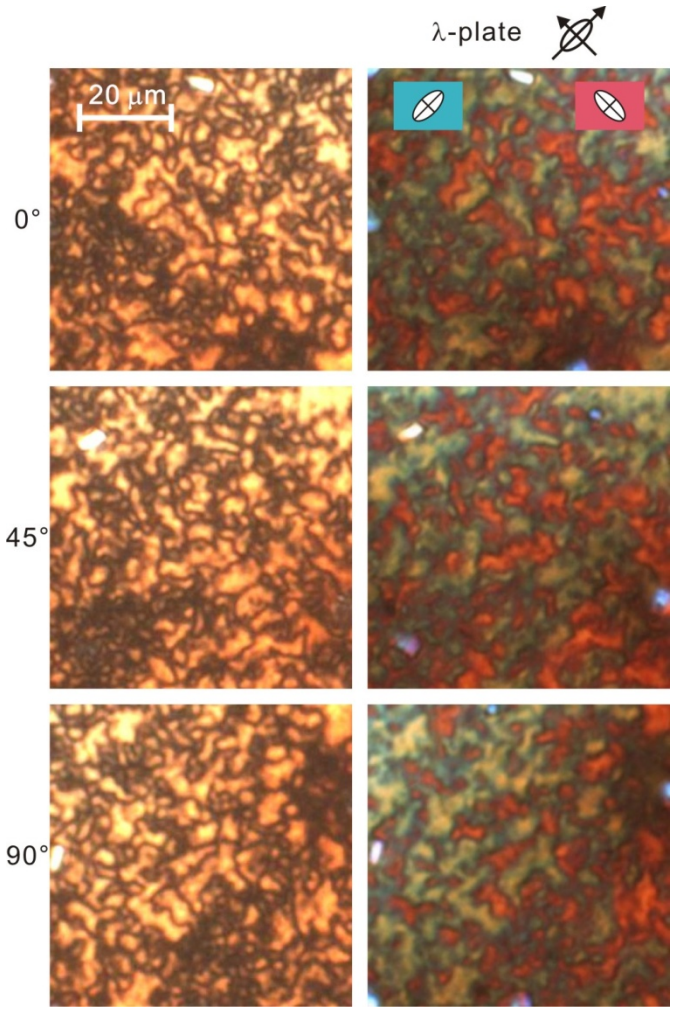

Figure S4. Textures of AuL3C6.

The Schlieren textures can be clearly seen in Figure S4. Without the λ-plate, the texture of the sample rotated by 90° is identical to that before the rotation (apart from the rotation of the image), while on rotation by 45°, the dark and bright regions exchanged positions. With the λ-plate in place, the blue and red regions exchange positions upon sample rotation by 90°, as one would expect.

6 TGA data of AuL3C12

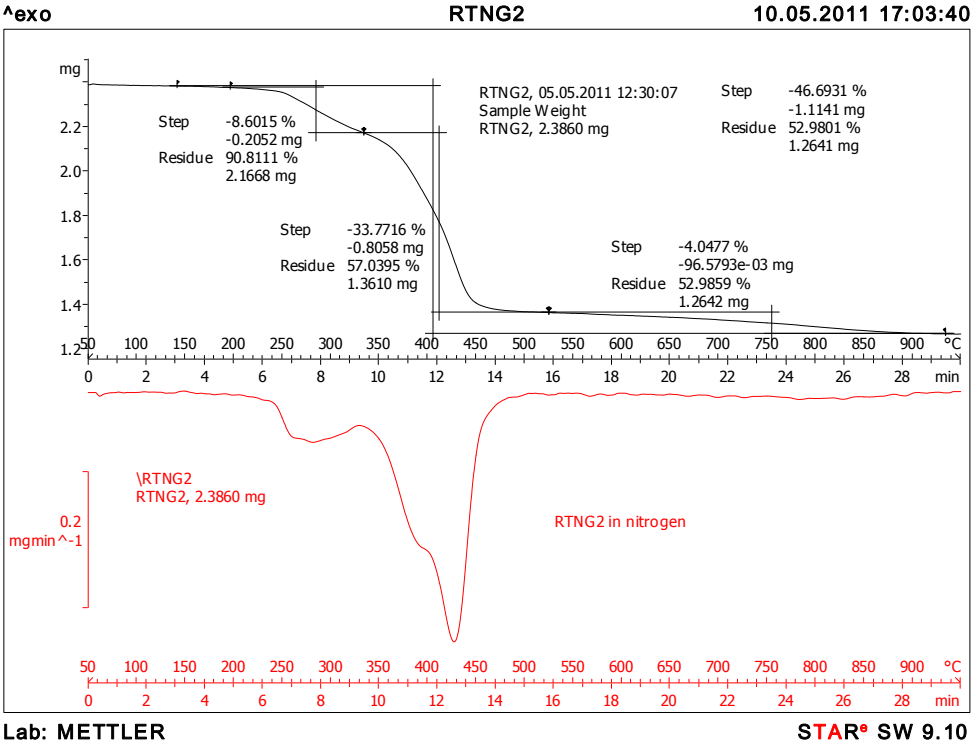

7 References

1. S. Diez, D. A. Dunmur, M. R de la Fuente, P. K. Karahaliou, G. Mehl, T. Mayer, M.A.P. Jubindo, D. J. Photinos, *Liq. Cryst.* 2003, **30**, 1021-1030.
2. B. Haché, Y. Gareau, *Tetrahedron Lett.* 1994, **35**, 1837-1840.
3. M. Brust, M. Walker, D. Bethell, D. J. Schiffrin, R. Whyman, *J. Chem. Soc. Chem. Comm.,* 1994, 801.
4. L. Cseh, G. H. Mehl, *J. Am. Chem. Soc.* 2006, **128**, 13377-13378.